

Robust detection and isolation of failures in satellite attitude sensors and gyro

Bahar Ahmadi and Mehrzad Namvar*

Department of Electrical Engineering, Sharif University of Technology, Tehran, Iran

(Accepted December 13, 2011. First published online: January 12, 2012)

SUMMARY

Reliability of a satellite attitude control system depends on accurate detection of failures in its sensors. This paper presents an observer for robust detection and isolation of a class of failures in satellite attitude sensors. The proposed observer uses measurement of a three-axis gyro together with only one attitude sensor, and generates a residual signal which is sensitive to faults and is simultaneously robust against disturbance and noise. A nonlinear model of satellite kinematics is considered for design of the observer. The structure of the observer is in the form of a delayed continuous-time differential equation ensuring its robustness properties. A realistic simulation is provided to illustrate the performance of the proposed observer in the face of the faults occurring in a magnetometer, as the attitude sensor, and also the faults occurring in the gyro.

KEYWORDS: Robotic self-diagnosis and self-repair; Navigation, Pose estimation and registration; Mobile robots, Automation.

1. Introduction

Accuracy and reliability of any satellite attitude control system relies on performance of the satellite attitude determination (AD) subsystem. However, despite all efforts for fault avoidance, occurrence of faults in navigational sensors such as rate gyros, magnetometers, Earth-horizon sensors, Sun sensors, or star trackers can significantly hinder the performance of the attitude determination system. A fault in an attitude sensor can be regarded as an unexpected change of sensor operation affecting the sensor output. Robust state observers are usually used in fault detection and isolation (FDI) systems to generate a *residual* signal that reacts to the presence of the fault and remains insensitive to disturbance and noise. Achieving this goal usually requires redundancy in the available information that can be physical or analytical.^{1,2} Despite its simplicity, hardware redundancy usually increases cost and weight, which in the case of the satellites with limited power and weight budget, does not seem practical. In contrast, analytical redundancy requires precise system modeling together with complex computations to acquire the residual signal.

Several approaches to robust fault detection and isolation for Linear Time Invariant (LTI) systems have been reported in

the literature which use optimization-based techniques such as Linear Matrix Inequality (LMIs) in order to minimize the effect of disturbances and simultaneously maximize the effect of faults on the residual signals.^{3–5} The same objective for the nonlinear Lipschitz systems was considered by Pertew *et al.*⁶ Sliding-mode observers were also employed for robust FDI for LTI systems by Tan and Edwards.⁷ However, assuming the satellite attitude matrix as the state and its angular velocity as the input, satellite kinematics can be regarded as a linear time-varying (LTV) system. So far, the FDI problem has been rarely investigated in literature for LTV systems. An optimal approach for robust fault detection for LTV systems was developed by Li and Zhou,⁸ where the main focus was on detection of faults; however, by using a bank of observers, the method can be used for isolation of faults as well.

Considerable research has been devoted to detection of faults for autonomous nonlinear systems in literature. A number of works achieved simultaneous detection and identification of faults by using the state observers that make the residual signal converge to the fault signal.^{9,10} A nonlinear observer with diagonal structure was proposed by Narasimhan *et al.*¹⁰ by assuming that faults were constant with respect to time. The LMI techniques were used by Yan and Edwards⁹ to develop a sliding-mode observer for robust detection and isolation of actuator faults. Moreover, Zhang *et al.*¹¹ used LMI-based sliding-mode observers to estimate sensor faults in the case of nonlinear Lipschitz systems but in the absence of disturbance signals. Xu and Zhang¹² and Yan and Edwards¹³ used adaptive techniques for fault detection in a certain class of nonlinear systems. An observer for single-output systems was proposed by Xu and Zhang,¹² where the faults were represented as elements of an unknown parameter vector. Despite the above researches, the effect of measurement noise was not generally considered. Namvar and Aghili¹⁴ proposed an FDI filter to deal with actuator and position faults in a robotic system without using velocity measurement and by taking into account the sensor noise.

In the case of satellite systems, the performance of the FDI systems can be evaluated based on the type and total number of used sensors, computational complexity, degree of assumptions on noise characteristics, and modeling accuracy. An FDI system based on the extended Kalman filtering (EKF) was presented by Pirmoradi *et al.*,¹⁵ where rate gyros together with two attitude sensors were used and it was assumed that at least one sensor was functioning without fault. The

* Corresponding author. E-mail: namvar@sharif.ir

fault signal was assumed to be added directly to the satellite Euler angles instead of attitude sensor outputs. Another approach for fault detection, based on the EKF innovation sequence, was proposed by Okatan *et al.*¹⁶ by using two attitude sensors and a rate gyro. Despite the use of Kalman filtering in satellite attitude determination being common, satellite kinematics and dynamics are nonlinear such that the EKF does not necessarily guarantees global asymptotic convergence of the estimation error to zero.¹⁷ In addition, stochastic assumptions on process and measurement noise are not satisfied in practice.

An observer-based scheme for detecting the faults in a rate gyro and a horizon sensor were presented by Venkateswaran *et al.*,¹⁸ where the linear model of satellite kinematics and dynamics was used, and measurement noise was ignored. Similarly, Gao *et al.*¹⁹ considered the fault as an unknown signal added directly to the Euler angles by using the linear model and ignoring sensor noise. Fault reconstruction together with detection and isolation of faults in attitude sensors and actuators were achieved using a sliding-mode observer in ref. [20] by using the linearized model of a satellite. Unfortunately, in most practical situations, the nonlinear properties of the satellite attitude dynamics and kinematics cannot be neglected in the fault diagnosis. For nonlinear systems, a novel fault detection scheme, using the unscented Kalman filter (UKF) was proposed by Xiong *et al.*²¹ and sufficient conditions for the convergence of the UKF were derived. The method was then applied to the satellite attitude determination system by assuming that measurements of sun sensor, earth sensor, and gyro were available. On the other hand, due to limitations in satellite weight and power budget, the use of small number of attitude sensors is desirable in practice. Consequently, the problem of detection and isolation of faults in satellite attitude sensors, by using only one attitude sensor and a single gyro, and taking into account the nonlinear model of satellite dynamics together with measurement noise, has remained open in literature.

In this paper, we use a rate gyro together with a single attitude sensor for detection and isolation of faults in the output of the attitude sensor. By using nonlinear attitude kinematics of the satellite, a novel third-order observer in form of a delayed differential equation is proposed such that the resulting residual signal is sensitive to sensor faults and simultaneously remains insensitive against measurement noise and disturbance. In the existing methods in literature, the residual signal at time t is directly affected by the value of disturbance at t . This usually results in high threshold level and low detection sensitivity. The use of delay in the proposed observer; however, makes the residual signal depend on the difference of the value of the disturbance signal at t and $t - h$, where h stands for the chosen delay. By proper choice of delay, this makes the residual signal significantly less sensitive to disturbance. Within a different framework, the use of delay has been shown to attenuate slowly-varying perturbations in the context of state feedback control.¹ The paper is organized as follows: Section 2 provides description of satellite dynamics. Section 3 describes the attitude sensor dynamics together with the assumptions and definitions related to the class of faults that can be isolated by the

proposed observer. Fault detection and isolation strategies are discussed in Section 4. Finally, simulation examples are presented in Section 6 illustrating the performance of the proposed FDI system in face of pulse-wise and ramp-wise faults in the output of a magnetometer, as well as a step-wise fault in the gyro.

2. Satellite Kinematics

We consider the satellite as a rigid body and assume a coordinate frame attached to the center-of-mass of the satellite. The rotational motion of the satellite can be described by²²

$$\dot{R} = -S(\omega)R, \tag{1}$$

where $R \in SO(3)$ is the rotation matrix of the Earth inertial frame with respect to the satellite body frame, while $\omega \in \mathbb{R}^3$ denotes the angular velocity of the satellite body frame with respect to the inertial frame and expressed in the body frame. Assuming that $\omega = [\omega_1, \omega_2, \omega_3]^T$, the skew operator is defined by

$$S(\omega) = \begin{pmatrix} 0 & -\omega_3 & \omega_2 \\ \omega_3 & 0 & -\omega_1 \\ -\omega_2 & \omega_1 & 0 \end{pmatrix}. \tag{2}$$

We assume that ω is measured by a three-axis rate gyro, and the rotation matrix R is unknown. Depending on the type of the used attitude sensors, we assume that a set of information denoted by the reference vector, $v_r \in \mathbb{R}^3$, is available numerically by means of astrophysical laws. For example, in case of using a sun sensor, v_r is a vector with its origin at Sun's location and its end at satellite position. In case of using a magnetometer, v_r is Earth's magnetic field vector evaluated at the satellite position in orbit. We assume that v_r is expressed with respect to the inertial frame. We denote the representation of the reference vector in the satellite body frame by $v_b \in \mathbb{R}^3$. The output of the attitude sensor gives measurement of v_b if no fault or noise is present in measurement. v_b and v_r are related by

$$v_b = Rv_r. \tag{3}$$

3. Problem Statement

The time derivative of $v_b(t)$ can be expressed by

$$\dot{v}_b = \dot{R}v_r + R\dot{v}_r. \tag{4}$$

By virtue of (1), we have $\dot{v}_b = -S(\omega)Rv_r + R\dot{v}_r$. Defining the disturbance signal $d \in \mathbb{R}^3$ as

$$d \triangleq R\dot{v}_r, \tag{5}$$

and $y(t) \in \mathbb{R}^3$ as the output of the attitude sensor, the attitude kinematics can be represented by

$$\dot{v}_b(t) = -S(\omega(t))v_b(t) + d(t), \tag{6}$$

$$y(t) = v_b(t) + n(t) + f_s(t), \tag{7}$$

where $n(t) \in \mathbb{R}^3$ denotes the measurement noise in the attitude sensor. The fault signal is considered as an unknown

but bounded signal denoted by $f_s(t) \in \mathbb{R}^3$. In this paper, detection and isolation of faults is realized by means of generation of a residual signal $r(t) \in \mathbb{R}^3$ such that each component of r is sensitive to a component of fault as stated by the following definition:⁶

Definition 1: Denoting the residual signal as $r(t)$ and the chosen threshold level by $T > 0$, fault detection and isolation is achieved if the residual remains below the threshold level when the fault is identically zero. Moreover, occurrence of fault implies that the residual surpasses the threshold level. Equivalently,

$$|r_i(t)| < T, \quad \text{if and only if } f_{s_i}(t) = 0.$$

for $i = 1, 2, 3$.

In the sequel, we consider the following assumptions:

Assumption 1: Faults do not occur simultaneously in any channel of the attitude sensor. However, if no fault occurs in gyro, then Assumption 1 is not necessary and simultaneous occurrence of faults in attitude sensor channels can be isolated.

Assumption 2: Constant and finite scalars c_v , c_f , and c_n exist such that

$$\|v_b\|_\infty < c_v, \quad \|f\|_\infty < c_f, \quad \|n\|_\infty < c_n,$$

where the infinite norm of a signal is defined by $\|u(t)\|_\infty = \sup_{t \geq 0} \|u(t)\|$. Besides, satellite angular velocity has a known upper bound $\bar{\omega}$ such that $\|\omega(t)\|_\infty < \bar{\omega}$.

3.1. Class of detectable faults in attitude sensors

Definition 2: For given $\zeta > 0$ and $\tau > 0$, and chosen constants $h > 0$ and $|\lambda| > 4\tau^{-1}$, we define the set \mathcal{F} by

$$\mathcal{F} = \left\{ f_{s_i} \in \mathbb{R} \mid f_{s_i}(t) = 0 \forall t < \tau \text{ and } \exists t_1 \in [\tau, \tau + h) : \right. \\ \left. |f_{s_i}(t_1)| - |\lambda| \int_\tau^{t_1} |f_{s_i}(s)| ds > \frac{\zeta}{|\lambda|} \right\}, \quad (8)$$

where f_{s_i} is the i th element of the fault signal $f_s(t)$.

Assumption 3: We assume that f_{s_i} belongs to \mathcal{F} .

Definition 2 specifies a class of fault signals that occur at the time $t = \tau$ and grow sufficiently fast within the time interval of length h . By virtue of Fig. 1, a time t_1 exists such that the amplitude of fault at t_1 is large enough that it overcomes the shaded area from τ to t_1 multiplied by $|\lambda|$.

Example 1: Step-wise faults: Assume that

$$f_{s_i}(t) = \begin{cases} a, & t \geq \tau, \\ 0, & t < \tau, \end{cases}$$

where $|a| > \frac{\zeta}{|\lambda|}$. It can be verified that for $t_1 = \tau$ the inequality (8) is satisfied, which means the step-wise fault can

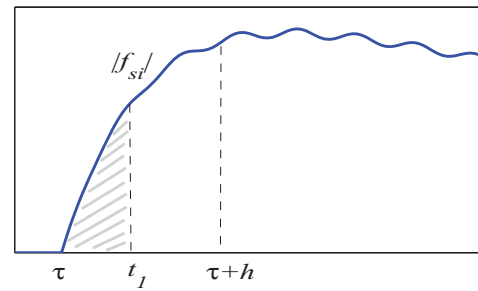


Fig. 1. (Colour online) Example of a fault belonging to the set \mathcal{F} . Here, τ denotes the time when fault occurs and t_1 is the detection time. h denotes the chosen delay time in the observer.

be immediately detected after its occurrence. The above explanation can be similarly repeated for the pulse-wise faults.

Note that the most common faults in the attitude sensors result from a sudden change of sensor measurements and can be modeled as step-wise signals.

Example 2: Ramp-wise faults: Let

$$f_{s_i}(t) = \begin{cases} \alpha(t - \tau), & t \geq \tau, \\ 0, & t < \tau, \end{cases}$$

where α is a scalar such that $|\alpha| \geq 2\zeta$. It can be shown that for t_1 belonging to the following interval:

$$t_1 \in \left[\tau + |\lambda|^{-1} (1 - \sqrt{\alpha^2 - 2\zeta|\alpha|}), \right. \\ \left. \tau + |\lambda|^{-1} (1 + \sqrt{\alpha^2 - 2\zeta|\alpha|}) \right] \quad (9)$$

the last inequality in Eq. (8) is satisfied. As a result, ramp-wise faults with sufficiently large slope fall into \mathcal{F} .

3.2. Class of detectable faults in gyro

Let a fault occur in the i th channel of the gyro and denote it by f_{ω_i} . Suppose that the fault occurs at $t = \tau_\omega$.

Definition 3: For given $\zeta_\omega > 0$ and $\tau_\omega > 0$, and chosen constant $|\lambda| > 4\tau_\omega^{-1}$, we define the set \mathcal{F}_ω by

$$\mathcal{F}_\omega = \left\{ \bar{f} \in \mathbb{R} \mid \bar{f}(t) = 0 \forall t < \tau_\omega \text{ and } \exists t_\omega \in [\tau_\omega, \tau_\omega + h) : \right. \\ \left. \left| \int_{\tau_\omega}^{t_\omega} e^{\lambda(t_\omega - s)} \bar{f}(s) ds \right| > \frac{\zeta_\omega}{|\lambda|} \right\}. \quad (10)$$

This definition specifies a class of faults that occur at $t = \tau_\omega$ and grow sufficiently fast in the interval of time $[\tau_\omega, t_\omega]$.

Assumption 4: We assume that for $j \neq i$, $\bar{f} = y_j f_{\omega_i}$ belongs to the set \mathcal{F}_ω . This means the output measurement y_j must not be zero in the interval $[\tau_\omega, \tau_\omega + h)$, i.e., after the occurrence of the fault f_ω .

Example 3: f_ω is a step-wise signal: We assume that the output signal $y_j(t)$ does not pass the zero in the time interval $[\tau_\omega, \tau_\omega + h]$. Let the term $\bar{f} = y_j(t) f_\omega(t)$ have the following

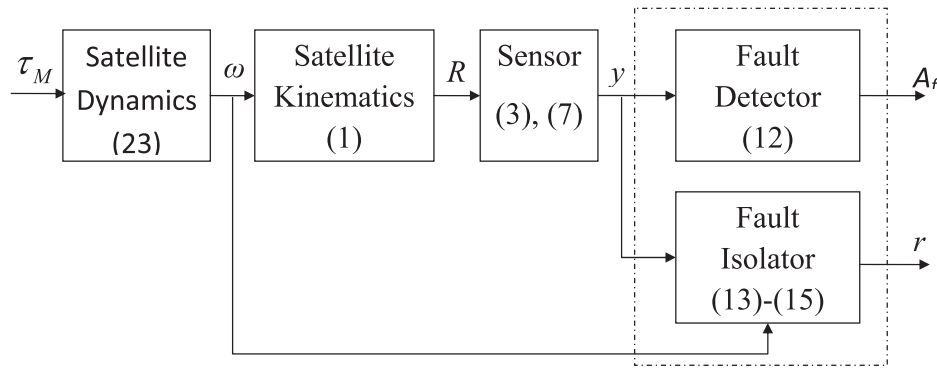


Fig. 2. Fault detection and isolation scheme.

form

$$\bar{f}(t) = \begin{cases} a(t), & t \geq \tau_\omega, \\ 0, & t < \tau_\omega, \end{cases}$$

where $a(t)$ is any bounded signal such that $|a(t)| > \zeta_\omega$ and $\min_t |a(t)| > 0$ for $t \in [\tau_\omega, \tau_\omega + h]$. For given values of h, λ, τ_ω , and ζ_ω , it can be shown that there exists t_ω at which the fault can be detected and by virtue of (10), t_ω is given by

$$t_\omega > \tau_\omega + |\lambda|^{-1} \ln \left(1 - \frac{\zeta_\omega}{\min_t a(t)} \right).$$

In a particular case, where $a(t) = y_j(t)$, a step-wise fault in f_ω can be handled, which shows that a step-wise fault in gyro belongs to \mathcal{F}_ω . Note that the introduction of the class of faults in (8) and (10) is justified due to the fact that most faults in the satellite attitude estimation system such as electronic short circuit, device saturation, data losses in the on-board computer or in the GPS, and gradual creation of bias in gyro measurement, can be modeled as pulse-wise or ramp-wise signals.

4. Fault Detection and Isolation in Attitude Sensors

Fault detection and isolation for satellite attitude sensors, with the dynamics model described by Eqs. (6) and (7), is discussed in this section (see Fig. 2).

4.1. Fault detection

Considering Eq. (7), it is inferred that

$$\|y\| \leq \|v_b\| + \|n\| + \|f\|. \tag{11}$$

Thus, by virtue of $v_b = Rv_r$, we have $\|v_b\| = \|v_r\|$, which yields

$$\text{if } f \equiv 0, \text{ then } \| \|y\| - \|v_r\| \| \leq c_n.$$

This concludes that the time when the fault occurs can be determined when the following inequality is satisfied:

$$\| \|y\| - \|v_r\| \| > c_n. \tag{12}$$

The output of the fault detector is then a pulse signal denoted by $A_f(t)$ that announces the presence of sensor fault.

However, isolation of faults needs further consideration and is discussed in the next section.

4.2. Fault isolation

We consider the following observer for isolation of attitude sensor faults:

$$\dot{z}(t) = Fz(t) + Fy(t-h) - (S(\omega(t)) + F)y(t) + S(\omega(t-h))y(t-h), \tag{13}$$

$$r(t) = z(t) + y(t-h) - y(t), \tag{14}$$

$$z(t_0) = z_0, \tag{15}$$

where $z, r \in \mathbb{R}^3$ are the state and output of the observer, respectively. The matrix $F \in \mathbb{R}^{3 \times 3}$ is a diagonal negative-definite matrix. The constant h is a free positive scalar representing the delay value in the delayed differential equation (13).²³ Also, z_0 denotes the initial condition. For simplicity, we set $F = \lambda I_3$ with $\lambda < 0$. The choice of λ determines the convergence time when the residual signal turns zero due to nonzero initial condition and in the absence of a fault signal. Moreover, we define the disturbance signal ϵ by

$$\epsilon(t) \triangleq (d(t-h) - d(t)) + (\dot{n}(t-h) - \dot{n}(t)) - (S(\omega(t-h))n(t-h) - S(\omega(t))n(t)) \tag{16}$$

and consider the following assumptions:

$$\|d(t-h) - d(t)\|_\infty < \delta_d(h), \tag{17}$$

$$\|S(\omega(t-h))n(t-h) - S(\omega(t))n(t)\|_\infty \leq \delta_n, \tag{18}$$

$$\|\dot{n}(t) - \dot{n}(t-h)\|_\infty \leq \delta'_n(h). \tag{19}$$

It is seen that $\|\epsilon(t)\|_\infty < c_\epsilon$, where

$$c_\epsilon \leq \delta_d(h) + \delta_n + \delta'_n(h). \tag{20}$$

Theorem 1: Let the fault f_s belong to the set \mathcal{F} and choose $\zeta = \bar{\omega}c_f + 2c_\epsilon$ in (8) where $\bar{\omega}, c_f$ are specified in Assumption 2. Define the threshold level T by

$$T = |\lambda|^{-1}(\bar{\omega}c_f + c_\epsilon). \tag{21}$$

If a fault occurs at the i th channel of the attitude sensor, then there exists a time $t_1 > 0$, where $|r_i(t_1)| > T$ while $|r_j(t)| < T$ for $t \geq t_1$ and $j \neq i$. \square

Proof: See Appendix A.

4.3. Selection of time delay h

Theorem 1 states that the occurrence of the fault can be isolated at the earliest time $t = t_1$. Since by definition $t_1 \leq \tau + h$, the delay h should be large enough to allow detection of the fault. For example, in the case of a ramp-wise fault in Example 3.1, for the detection time t_1 to exist, it is necessary to have $h > |\lambda|^{-1}(1 - \sqrt{\alpha^2 - 2\zeta|\alpha|})$, which means the delay needs to be kept higher than certain value. Moreover, when noise level in sensors is high, ζ as specified by Theorem 1, is large and as a result the delay h should be kept large. In general, large h means large class of detectable faults. On the other hand, by virtue of Eqs. (17)–(19), the value of delay is limited from above. From the residual equation (34), it is clear that the residual $r_i(t)$ is affected by both the fault and the disturbance $\epsilon_i(t)$. However, the disturbance signal, defined by Eq. (20), depends only on the differences of some time-dependent signals evaluated at t and $t - h$. Hence, a small delay results in a small disturbance and consequently a small threshold level. In the sequel, we present two examples to highlight this issue.

4.3.1. Case study. We aim to calculate the upper bounds $\delta_d(h)$ and $\delta'_n(h)$ as defined by Eqs. (17) and (20). Consider the case of using a magnetometer as attitude sensor. The Earth magnetic vector with respect to the orbital frame is approximately given by

$$v_r^o = \begin{pmatrix} \mu_f r_o^{-3} \sin(i) \cos(\omega_0 t) \\ -\mu_f r_o^{-3} \cos(i) \\ 2\mu_f r_o^{-3} \sin(i) \sin(\omega_0 t) \end{pmatrix},$$

where $\mu_f = 7.9 \times 10^{15}$ Wb.m⁻¹ denotes the magnetic field dipole strength, t represents time, r_o is the orbital circular radius, and i denotes the orbit inclination. The orbital angular velocity ω_0 is in the order of 0.001 rad/s at an altitude of 700 Km. In this case, the modeled disturbance signal $d(t)$ is given by

$$d = R_o^b \dot{v}_r^o = R_o^b \begin{pmatrix} -\mu_f r_o^{-3} \omega_0 \sin(i) \sin(\omega_0 t) \\ 0 \\ 2\mu_f r_o^{-3} \sin(i) \omega_0 \cos(\omega_0 t) \end{pmatrix}, \quad (22)$$

where R_o^b denotes the orientation of the body frame with respect to the orbit. Obviously, the variation of $d(t)$ depends on ω_0 . It can be shown that

$$\|\dot{d}\| \leq (2\mu_f r_o^{-3} \omega_0 |\sin(i)|)(\bar{\omega} + \omega_0) := A.$$

On the other hand, we know that $\|d(t) - d(t - h)\| \leq \|\dot{d}\|h + O(h^2)$, where $O(h^2)$ can be neglected for a small delay. Consequently, $\delta_d(h)$ is calculated by $\delta_d(h) = Ah$, which shows that a small delay results in a small upper bound for the disturbance in difference form. Next, we calculate

$\delta'_n(h)$ in case of a twice differentiable noise $n(t)$. Assuming that delay is sufficiently small, it can be shown that

$$\|\dot{n}(t) - \dot{n}(t - h)\| \leq \max_{t-h \leq \zeta \leq t} \|\ddot{n}(\zeta)\|h := \delta'_n(h). \quad (23)$$

Assume, for example, that $n(t)$ is a result of filtering of a bounded disturbance as $n = G(s)w$, where $G(s)$ is a strictly stable system of relative degree higher than 1, and $w(t)$ is a bounded disturbance with $\|w(t)\|_\infty \leq 1$. Then, $\|\ddot{n}(t)\|_\infty \leq \|s^2 G(s)\|_1$ such that $\|\dot{n}(t) - \dot{n}(t - h)\| \leq \|s^2 G(s)\|_1 h := \delta'_n(h)$. Once again, it is seen that the upper bound for the difference term $\dot{n}(t) - \dot{n}(t - h)$ can be significantly reduced if delay is kept small.

4.4. Effect of gyro noise on detection of attitude sensor faults

Lemma 1: Let us denote the measured angular velocity of satellite by ω_m which is contaminated by the additive noise n_ω ,

$$\omega_m = \omega + n_\omega. \quad (24)$$

Consider the observer (13)

$$\begin{aligned} \dot{z}(t) &= Fz(t) + Fy(t - h) - (S(\omega_m(t)) + F)y(t) \\ &\quad + S(\omega_m(t - h))y(t - h). \end{aligned}$$

Assuming that \bar{c}_n is a known upper bound for gyro noise such that

$$\|n_\omega\|_\infty \leq \bar{c}_n \quad (25)$$

and

$$\|S(n_\omega(t - h))y(t - h) - S(n_\omega(t))y(t)\|_\infty \leq c_\gamma. \quad (26)$$

Then, the threshold level is given by

$$T = |\lambda|^{-1}(\bar{\omega}_m c_f + c_\epsilon + c_\gamma), \quad (27)$$

where the term ζ is given by $\zeta = \bar{\omega}_m c_f + 2c_\epsilon + 2c_\gamma$ and $\bar{\omega}_m = \bar{\omega} + \bar{c}_n$ and c_γ is defined by

$$c_\gamma = 2\bar{c}_n(c_v + c_f + c_n). \quad (28)$$

Proof: See Appendix B.

4.5. Detection of fault clearance

In this section, we discuss a procedure to determine when a fault in the attitude sensors is cleared. Recall that τ is the time when a fault occurs. Also, t_1 is the time when a fault is detected and isolated. We define τ' and t'_1 as the instants of time when a fault is actually cleared and its clearance is determined, respectively. For any $\tau' > t_1 + h + 4|\lambda|^{-1}$, let

us define the extended class of faults by

$$\bar{\mathcal{F}} = \left\{ f_{s_i}(t) \in \mathcal{F} \mid f_{s_i} = 0 \forall t > \tau' \text{ and } \exists t'_1 \in [\tau', \tau' + h) : \right.$$

$$\left. |f_{s_i}(t'_1 - h)| - |\lambda| \int_{\tau'}^{t'_1} |f_{s_i}(s - h)| ds > \frac{\zeta}{|\lambda|} \right\}, \quad (29)$$

$$\left. |f_{s_i}(t'_1 - h)| - |\lambda| \int_{\tau'}^{t'_1} |f_{s_i}(s - h)| ds > \frac{\zeta}{|\lambda|} \right\}, \quad (30)$$

where the values of h , λ , and ζ are known. Moreover, we assume that $\hat{f}_{s_i}(t)$ is a smooth function for $\tau + h < t < \tau' - h$, such that $\|\hat{f}_{s_i}(t) - \hat{f}_{s_i}(t - h)\|_\infty \leq \delta'_f(h) \leq \bar{\omega}c_f$.

Theorem 2: Consider the observer introduced by Eqs. (13)–(15). Assume that faults belong to the class $\bar{\mathcal{F}}$. Assume that there exists a time $t = t'_1 > t_1 + h + 4|\lambda|^{-1}$, where the residual signal surpasses the threshold, i.e., $|r_i(t'_1)| > T$. Then, $f_{s_i}(t) = 0 \forall t > t'_1$.

Proof of this theorem is similar to the proof of Theorem 1.

Remark 1: Note that due to smoothness of \hat{f}_{s_i} , the condition $\tau' > t_1 + h + 4|\lambda|^{-1}$ states that the residual signal has converged to a close vicinity of zero before the time t'_1 , i.e., $|r_i(t)| < T$ for $t < t'_1$.

5. Fault Detection and Isolation for Gyro

Denote $\omega_m \in \mathbb{R}^3$ as the measured angular velocity by a gyro such that

$$\omega_m = \omega + n_\omega + f_\omega,$$

where n_ω is the measurement noise, and f_ω denotes the fault occurring in gyro. Define the disturbance ε by

$$\varepsilon \triangleq c_\varepsilon + S(n_\omega(t - h))y(t - h) - S(n_\omega(t))y(t).$$

Then, $\|\varepsilon\|_\infty \leq c_\varepsilon$, where

$$c_\varepsilon = c_\varepsilon + c_\gamma$$

and $c_\gamma \leq 2\bar{c}_n(c_v + c_n)$, where c_ε is given by (20). According to Assumption 1, we assume that no fault occurs in attitude sensors, i.e., $f_s(t) = 0$.

Theorem 3: Assume that $\bar{f} = f_\omega y_j$ belongs to the set \mathcal{F}_ω , where $\zeta_\omega = 2c_\varepsilon$ in Eq. (10). Consider the observer introduced by Eqs. (13)–(15) and define the threshold level T by

$$T = |\lambda|^{-1}c_\varepsilon. \quad (31)$$

If a fault occurs at the i th channel of a gyro, then there exists a time $t_\omega > 0$, where $|r_j(t)|$ surpasses the threshold for $j \neq i$, i.e., $|r_j(t)| > T$, while $|r_i(t_1)| < T$ for $\forall t$.

Proof: See Appendix C.

By Theorem 3 we infer that the occurrence of a fault in the i th channel affects all residuals except the i th residual.

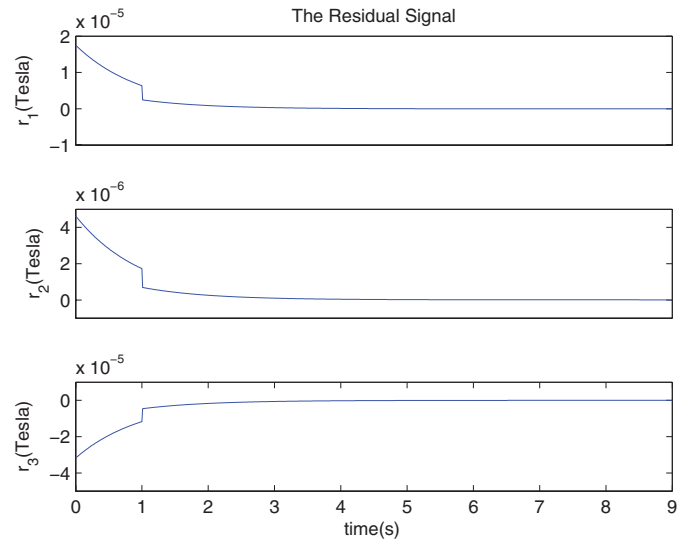


Fig. 3. (Colour online) Transient response of residuals when no fault occurs. Residuals tend to zero asymptotically.

6. Simulation Results

We consider a rigid satellite with kinematics described by Eq. (1), and the dynamics given by

$$\tau_M = I\dot{\omega} + \omega \times I\omega, \quad (32)$$

where τ_M is the external torque expressed in the body frame, and $I \in \mathbb{R}^{3 \times 3}$ is the constant moment-of-inertia matrix of the satellite given by $I = \text{diag}(13.654, 13.555, 0.765)$ Kg.m². The satellite is assumed to be moving in the sun-synchronous orbit with the inclination of 60°, the altitude of 540 Km, zero right ascension of the ascending node and argument of perigee, and the 1.68×10^{-4} of eccentricity.

Gravity gradient boom is considered as the only source of external torque to the satellite.²⁴ We consider a magnetometer as the attitude sensor, where its output is modeled by $y = v_b + \bar{n}$, where y is the measured sensor output and v_b is the actual magnetic field expressed in the body frame. Moreover, \bar{n} denotes the output disturbance given by $\bar{n} = n + S(e)v_b$, where n is considered as a filtered uniform random number with the upper bounds $c_n = 10^{-7}$ Tesla and $c'_n = 10^{-7}$ Tesla/s, and e is the magnetometer misalignment vector. For modeling the magnetic field vector in the inertial frame, we use the International Geomagnetic Reference Field (IGRF) model.²⁵ We consider an additive uniform random number together with a constant bias for the gyro measurement such that $\bar{c}_n \leq 10^{-5}$ rad/s (2.06 deg/h) in Eqs. (24) and (25). We assume the initial condition of the observer (13)–(15) as $z(t_0) = [0, 0, 0]^T$. The upper bound for the magnetometer fault amplitude c_f is assumed as 10^{-5} Tesla. Also, we consider the delay value $h = 1$ s and the residual response time $\lambda = 1$. This leads us to the threshold level of $T = 8 \times 10^{-8}$ Tesla according to Eq. (27).

Performance of the observer in the absence of faults is shown in Fig. 3. Obviously, before occurrence of the fault, the residual signal converges to a close vicinity of zero. Figure 4 shows the residual response to a step-wise and also a ramp-wise fault in the first channel of the magnetometer. The step-wise fault with the amplitude of 10^{-5} Tesla starts at

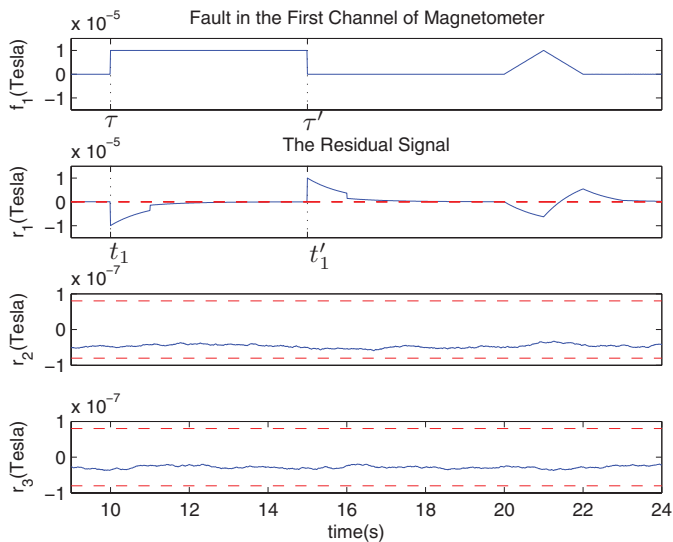


Fig. 4. (Colour online) Residuals when fault occurs in magnetometer first channel (solid). Threshold level (dash). Sensitivity of r_1 is an indication that f_1 has occurred.

$t = \tau = 10$ s and ends at $t = \tau' = 15$ s; in addition, the ramp-wise fault occurs at time $t = \tau = 10$ s with the amplitude of 10^{-5} Tesla and the rate of 10^{-5} Tesla/s. It is observed that the first element of the residual signal $r_1(t)$ exceeds the threshold level at time $t = t_1$. In light of Theorem 2, the clearance of the step-wise fault is identified at time $t'_1 \approx 15$ s.

Next, as another scenario, we assume a pulse-wise fault with the amplitude of 10^{-2} rad/s occurring in the gyro's second channel. Figure 5 shows the residual signal together with the threshold level of $T = 5 \times 10^{-8}$ Tesla. As predicted by Theorem 3, $r_1(t)$ and $r_3(t)$ exceed the threshold level and r_2 remains insensitive to fault.

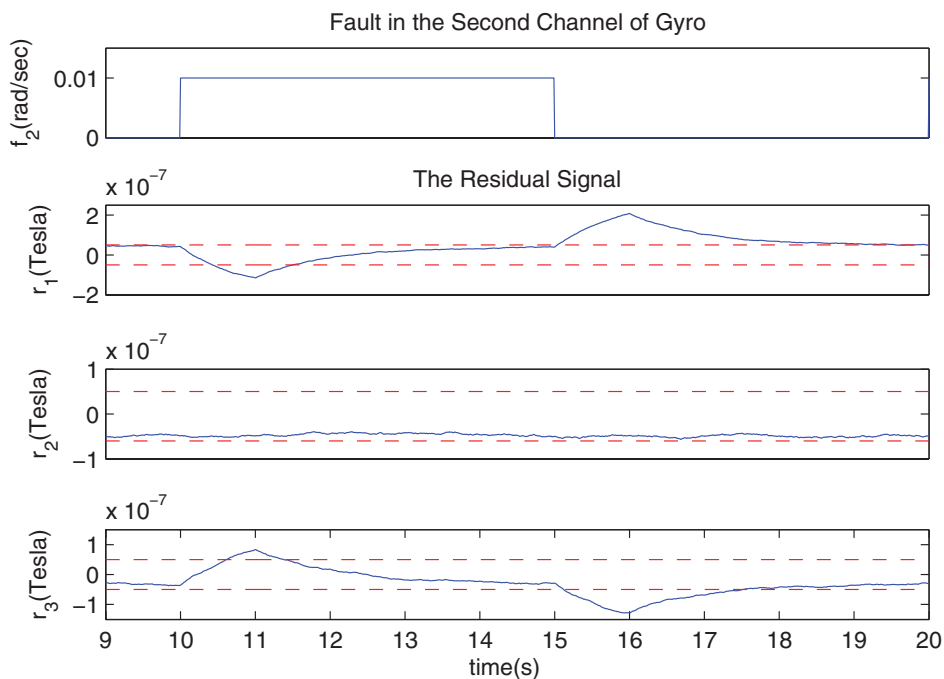


Fig. 5. (Colour online) Residual signals in response to a fault in gyro's second channel (solid). Threshold levels (dash). Insensitivity of the residual r_2 is an indication that f_2 has occurred.

6.1. Comparison with non-delay-based approaches

For comparison purpose, the sliding-mode fault detector of Chen and Saif²⁶ was implemented for the satellite system. The residual dynamics in response to the fault f_{s_i} is given by

$$\dot{r}_i = \lambda r_i - \eta \text{sgn}(r_i) + \epsilon_i - \dot{f}_{s_i},$$

where ϵ_i represents the effect of disturbance and sensor noise. Also, $\eta > 0$ is chosen such that $\eta > \|\epsilon\|_\infty$. The important difference between ϵ_i here with ϵ_i defined in (16) is that here ϵ_i depends on disturbance and noise at time t . As a result, when disturbance is not negligible and its magnitude is comparable to the fault, its effect is indistinguishable from the effect of the fault. In contrast, the use of the delayed-based observer (13) transforms the residual dynamics into Eq. (34), i.e.,

$$\dot{r}_i = \lambda r_i + \epsilon_i - \dot{f}_{s_i},$$

where by virtue of Eq. (16) the perturbation ϵ_i is a difference of time varying functions. Based on the discussions in Section 4.3, the upper bound for the disturbance depends on the delay h and can be made small by choosing a small delay. Figure 6 illustrates the response of two methods to a step-wise fault occurring in the second channel of the magnetometer at time $t = 10$ s, and with the amplitude of 10^{-6} Tesla. The fault was not detected by the non-delay-based sliding-mode method because the effect of fault was lost in the residual signal. However, the proposed observer effectively detects and isolates the fault.

7. Conclusions

A new scheme for fault detection and isolation in satellite gyro and attitude sensors was proposed. The class of

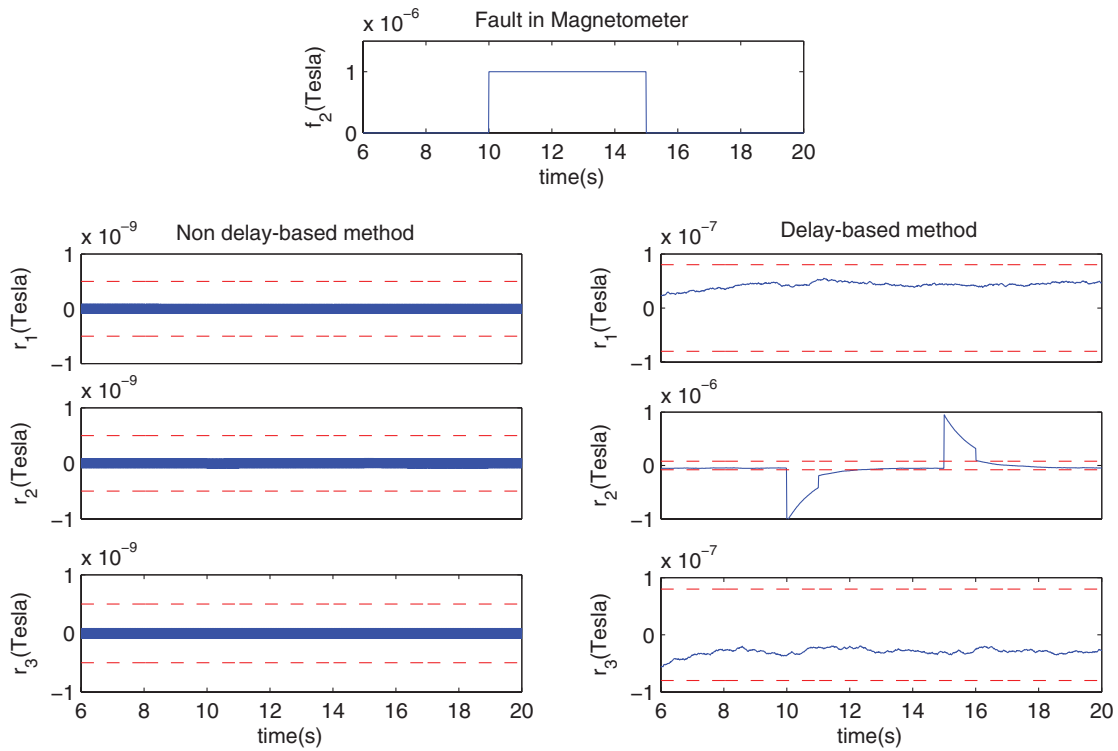


Fig. 6. (Colour online) Residual signals for a non-delay-based sliding-mode method (left column) in comparison with the proposed delay-based observer (right column) in the presence of sensor noise. Fault occurs in the second channel of magnetometer at $t = 10$ s.

detectable faults was shown to include most common forms of fault signals. Based on the nonlinear model of the satellite, the proposed observer used only a three-axis gyro and a single attitude sensor. The structure of the observer was in the form of a delayed differential equation. Use of delay in the observer was shown to reduce the sensitivity of residuals to noise.

Appendix

A. Proof of Theorem (1)

When a fault occurs at $t = \tau$ in the i th element of the attitude sensor, the residual signal is given by

$$\begin{aligned} \dot{r}(t) = & Fr(t) + \epsilon(t) + (\dot{f}(t - h) - \dot{f}(t)) \\ & + (S(\omega(t - h))f(t - h) - S(\omega(t))f(t)). \end{aligned} \quad (33)$$

Since $F = \lambda I$ with $\lambda < 0$, the residual signal is bounded, i.e., $r(t) \in \mathcal{L}_\infty$. Based on Eq. (33), as long as $t - h < \tau$, the terms $\dot{f}(t - h)$ and $S(\omega(t - h))f(t - h)$ are zero. Therefore, Eq. (33) simplifies into

$$\dot{r}_i(t) = \lambda r_i + \epsilon_i(t) - \dot{f}_{s_i}(t), \quad (34)$$

$$\dot{r}_j(t) = \lambda r_j + \epsilon_j(t) - S_{ji}(t)f_{s_i}(t), \quad \forall i \neq j, \quad (35)$$

where S_{ji} denotes the (j, i) th element of the matrix $S(\omega)$. Notice that \dot{f}_{s_i} affects \dot{r}_i directly, whereas S_{ji} reduces the effects of f_{s_i} on \dot{r}_j (Due to the fact that S_{ji} depends on the satellite angular velocity whose magnitude is normally smaller than 1 rad/s; however, the proof does not rely on this assumption). We assume that the residual transient response to nonzero initial condition has passed, and faults occur after

this transient period. Now, consider the Lyapunov function $V_j = 1/2r_j^2$. Then,

$$\dot{V}_j = \lambda r_j^2 + (\epsilon_j - S_{ji}f_{s_i})r_j \leq |r_j|(|\lambda|r_j + |\epsilon_j - S_{ji}f_{s_i}|),$$

which is negative for $|r_j| > \frac{(|\epsilon_j - S_{ji}f_{s_i}|)}{|\lambda|}$. Hence, $r_j(t)$ is bounded by

$$|r_j| < (c_\epsilon + \bar{\omega}c_f)|\lambda|^{-1}.$$

Therefore, the inequality $|r_j| < T$ is always satisfied. Now, considering the dynamics equation (34) leads us to

$$\begin{aligned} r_i(t) = & \int_0^t e^{\lambda(t-s)}(\epsilon_i(s) - \dot{f}_{s_i}(s)) ds \\ = & \int_0^t e^{\lambda(t-s)}\epsilon_i(s)ds + \int_0^t e^{\lambda(t-s)}(-\dot{f}_{s_i}(s)) ds \\ = & r_{i1}(t) + r_{i2}(t). \end{aligned}$$

It is obvious that $|r_{i1}(t)| \leq \frac{c_\epsilon}{|\lambda|}$. For $r_{i2}(t)$, we have

$$r_{i2}(t) = -f_{s_i}(t) - \lambda \int_0^t f_{s_i}(s) e^{\lambda(t-s)} ds.$$

Obviously,

$$\left| |f_{s_i}(t)| - \left| \lambda \int_0^t f_{s_i}(s) e^{\lambda(t-s)} ds \right| \right| \leq |r_{i2}(t)|.$$

Since

$$\left| \int_0^t f_{s_i}(s) e^{\lambda(t-s)} ds \right| \leq \int_0^t |f_{s_i}(s)| ds, \tag{36}$$

it is implied that

$$|f_{s_i}(t)| - |\lambda| \int_0^t |f_{s_i}(s)| ds \leq |r_{i2}(t)|.$$

Now, according to Assumption 3, at time $t = t_1$ and for $\zeta = \bar{\omega}c_f + 2c_\epsilon$, we have

$$\frac{\bar{\omega}c_f + 2c_\epsilon}{|\lambda|} < |r_{i2}(t_1)|. \tag{37}$$

On the other hand, the residual signal $r_i(t)$ always satisfies

$$||r_{i2}(t)| - |r_{i1}(t)|| \leq |r_i(t)|.$$

Hence, at time $t = t_1$, we have

$$\left| \frac{\bar{\omega}c_f + 2c_\epsilon}{|\lambda|} - \frac{c_\epsilon}{|\lambda|} \right| \leq |r_i(t_1)|,$$

which finally implies

$$T \leq |r_i(t_1)|.$$

B. Proof of Lemma 1

Considering the noise in gyro changes the residual dynamics into

$$\dot{r}(t) = Fr(t) + \epsilon(t) + S(n_\omega(t-h))y(t-h) - S(n_\omega(t))y(t).$$

Note that for the largest singular value of the matrix $S(n)$, denoting by $\bar{\sigma}(S(n))$, we have $\bar{\sigma}(S(n)) \leq \bar{c}_n$. This yields, $c_\gamma = 2\bar{c}_n \|y(t)\|_\infty$. Since

$$\|y(t)\| \leq c_v + c_f + c_n,$$

hence c_γ is given by Eq. (28).

C. Proof of Theorem(3)

When the fault in the i th element of gyro occurs, the residual signal changes into

$$\dot{r}(t) = Fr(t) + \epsilon(t) + S(y(t-h))f_\omega(t-h) - S(y(t))f_\omega(t). \tag{38}$$

Based on Eq. (38), as long as $t-h < \tau_\omega$, the term $f_\omega(t-h)$ is zero. Moreover, denoting $\bar{f} = y_j f_\omega$, Eq. (33) can be simplified by

$$\dot{r}_i(t) = \lambda r_i + \epsilon_i(t), \tag{39}$$

$$\dot{r}_j(t) = \lambda r_j + \epsilon_j(t) - \bar{f}_{\omega_i}(t), \quad \forall i \neq j. \tag{40}$$

It is clear that $|r_i| < \frac{c_\epsilon}{|\lambda|}$ and we always have $|r_i| < T$. Now, the dynamics equation (40) yields

$$\begin{aligned} r_j(t) &= \int_0^t e^{\lambda(t-s)} \epsilon_j(s) ds + \int_0^t e^{\lambda(t-s)} (-S_{ji}(y(s)) f_{\omega_i}(s)) ds \\ &= r_{j1} + r_{j2}, \end{aligned}$$

where $|r_{j1}(t)| \leq \frac{c_\epsilon}{|\lambda|}$. On the other hand,

$$\left| \int_0^t e^{\lambda(t-s)} \bar{f}_{\omega_i}(s) ds \right| \geq \frac{\zeta_\omega}{|\lambda|}.$$

According to assumption (4), at time $t = t_\omega$ and for $\zeta_\omega = 2c_\epsilon$, we conclude that

$$|r_j(t_\omega)| \geq T.$$

References

1. P. M. Frank, "Fault diagnosis in dynamic systems using analytical and knowledge based redundancy, a survey and some new results," *Automatica* **26**(3), 459–474 (1990).
2. R. Patton, P. Frank and R. Clark, *Fault Diagnosis in Dynamic Systems: Theory and Applications* (Prentice-Hall, Englewood Cliffs, NJ, 1989).
3. A. Casavola, D. Famularo and G. Franz, "A robust deconvolution scheme for fault detection and isolation of uncertain linear systems: An LMI approach," *Automatica* **41**, 1463–1472 (2005).
4. M. Zhong, S. X. Ding, J. Lam and H. Wang, "An LMI approach to design robust fault detection filter for uncertain LTI systems," *Automatica* **39**, 543–550 (2003).
5. J. Liu, J. L. Wang and G. H. Yang, "An LMI approach to minimum sensitivity analysis with application to fault detection," *Automatica* **41**, 1995–2004 (2005).
6. A. M. Pertew, H. J. Marquez and Q. Zhao, "LMI-based sensor fault diagnosis for nonlinear Lipschitz systems," *Automatica* **43**, 1464–1469 (2007).
7. C. P. Tan and C. Edwards, "Sliding mode observers for detection and reconstruction of sensor faults," *Automatica* **38**, 1815–1821 (2002).
8. X. Li and K. Zhou, "A time domain approach to robust fault detection of linear time-varying systems," *Automatica* **45**, 94–102 (2009).
9. X. G. Yan and C. Edwards, "Fault Reconstruction/Estimation Using a Sliding Mode Observer," *Proc. of the IEEE Conference on Decision and Control*, San Diego, USA (2006) pp. 5573–5578.
10. S. Narasimhan, P. Vachhani and R. Rengaswamy, "New nonlinear residual feedback observer for fault diagnosis in nonlinear systems," *Automatica* **44**, 2222–2229 (2008).
11. K. Zhang, S. Hu and B. Jiang, "Sliding mode integral observers for sensor faults detection and isolation in nonlinear systems," *Proc. of the IEEE International Conference on Control and Automation*, Singapore, Malaysia (2007) pp. 147–151.
12. A. Xu and Q. Zhang, "Nonlinear system fault diagnosis based on adaptive estimation," *Automatica* **40**, 1181–1193 (2004).
13. X. G. Yan and C. Edwards, "Adaptive sliding-mode-observer-based fault reconstruction for nonlinear systems with parametric uncertainties," *IEEE Trans. Ind. Electron.* **55**(11), 4029–4036 (2008).
14. M. Namvar and F. Aghili, "Failure detection and isolation in robotic manipulators using joint torque sensors," *Robotica* **28**, 549–561 (2009).
15. F. N. Pirmoradi, F. Sassani and C. W. de Silva, "Fault detection and diagnosis in a spacecraft attitude determination system," *Acta Astronaut.* **65**, 710–729 (2009).

16. A. Okatan, C. Hajiyeve and U. Hajiyeve, "Kalman filter innovation sequence based fault detection in LEO satellite attitude determination and control system," *Recent Adv. Space Technol.* 411–416 (2007).
17. B. D. O. Anderson and J. B. Moore, *Optimal Filtering* (Prentice-Hall, Englewood Cliffs, NJ, 1979).
18. N. Venkateswaran, M. S. Siva and P. S. Goel, "Analytical redundancy based fault detection of gyroscopes in spacecraft applications," *Acta Astronaut.* **50**(9), 535–545 (2002).
19. Z. Gao, B. Jiang, P. Shi and Y. Cheng, "Sensor fault estimation and compensation for microsatellite attitude control systems," *Int. J. Control Autom. Syst.* **8**(2), 228–237 (2010).
20. L. Wu, Y. Zhang and H. Li, "Research on fault detection for satellite attitude control systems based on sliding mode observers," *Proc. of the IEEE International Conference on Mechatronics and Automation*, Changchun, Jilin, China (2009) pp. 4408–4413.
21. K. Xiong, C. W. Chan and H. Y. Zhang, "Detection of satellite attitude sensor faults using the UKF," *IEEE Trans. Aerosp. Electron. Syst.* **43**(2), 480–491 (2007).
22. M. Spong, S. Hutchinson and M. Vidyasagar, *Robot Modeling and Control*. (John Wiley and Sons, Hoboken, NJ, 2006).
23. J. P. Richard, "Time-delay systems: An overview of some recent advances and open problems," *Automatica* **39**, 1667–1694 (2003).
24. M. J. Sidi, *Spacecraft Dynamics and Control*. (Press Syndicate of the University of Cambridge, New York, 1997).
25. N. Olsen, T. J. Sabaka and L. T. Clausen, "Determination of the IGRF 2000 model," *Earth Planets Space* **52**, 1175–1182 (2000).
26. W. Chen and M. Saif, "Robust fault detection in uncertain nonlinear systems via a second order sliding mode observer," *Proceedings of the 40th IEEE Conference on Decision and Control*, Orlando, Florida, USA (2001) vol. 1, pp. 573–578.